SubjuGator: Sink or Swim?

Jennifer L. Laine, Scott A. Nichols, David K. Novick, Patrick D. O'Malley, Ivan Zapata, Michael C. Nechyba and Antonio Arroyo

Machine Intelligence Laboratory
University of Florida
Gainesville, FL 32611-6200

http://mil.ufl.edu/subjugator

Abstract

Undergraduate and graduate students at the University of Florida have completely redesigned, modified and tested an autonomous submarine, SubjuGator, to compete in the 2000 ONR/AUVSI Underwater Vehicle Competition. SubjuGator is designed for operation down to 100 feet, and can be quickly configured to optimize for mobility or speed. SubjuGator's body, sleeker than our previous entries, has mounts to support up to ten motors, each of which may be oriented in any direction in its plane. For the competition, we will mount six motors in sets of two, where each set is orthogonal to the others. SubjuGator is controlled through a single-board 586 computer running the Linux operating system, which is interfaced to the motors and sensors through two other processors, a DSP and a microcontroller. On-board sensors include a digital compass, fluidic inclinometer, sonar altimeter and a pressure sensor. Additionally, mission-specific sensors include a hydrophone array for acoustic ping detection and localization, a CdS array for visual strobe detection and localization, and a camera for target-hoop acquisition. In this paper, we first describe the mechanical makeup of SubjuGator. Next, we describe the electronic and processing hardware, and the motivation for our electronic design. We then discuss the various on-board sensors, both mission-dependent as well as mission-independent. Finally, we briefly comment on how we expect a typical competition run to proceed and how the subsystems on board SubjuGator will allow us to meet the mission goals.

1. Introduction

The Autonomous Unmanned Vehicle Systems International (AUVSI) and the U.S. Office of Naval Research (ONR) are sponsoring the Third Annual Autonomous Underwater Vehicle Competition to be held in Orlando, July 7-9, 2000. A student team at the University of Florida, mostly veterans of the first two competitions, are once again developing an AUV for this latest contest. SubjuGator has been completely redesigned to improve on previous efforts and to meet the more difficult challenges of this year's competition.

This year, the submarine must navigate a pond in search of a beacon emitting acoustic and visual pulses, activated at the start of the mission. Points are awarded for determining the flash rate of the beacon strobe, the ping rate of the acoustic pulse, and retrieval of a hoop located at the beacon site. All of this must happen autonomously. Our redesigned SubjuGator vehicle has been developed in part to meet these challenges.

In this paper, we first describe the mechanical makeup of SubjuGator. Next, we describe the electronic and processing hardware, and the motivation for our electronic design. We then discuss the various on-board sensors, both mission-dependent as well as mission-independent. Finally, we briefly comment on how we expect a typical competition run to proceed and how the subsystems on board SubjuGator will allow us to meet the mission goals.

2. Mechanical System

As a third-generation vehicle, SubjuGator embodies the lessons learned in three years of autonomous underwater vehicle (AUV) development. We considered several key design criteria, including the vehicle's hydrodynamics, its survivability in a salt-water environment, and its adaptability for different missions through easy motor reconfiguration and future sensor additions.

2.1 Body

The 36" long octagonal shape is composed of 0.25" thick aluminum plate and 0.5" thick square bar. A bulkhead on each end fastened with quick-release latches keeps the internals dry, while allowing access to the components from either end of the sub. Three hardpoint rings are welded onto the frame (Figure 1) to strengthen the structure, provide mounting points for exterior sensors via blind-tapped holes, and carry all through-hull connections. The central hardpoint ring also contains the cylindrical mounts for eight motors. The mount allows the motor's thrust to be positioned in line with the body, or perpendicular to it. With a mount on each of the eight faces of the sub, a multitude of motor configurations are possible, allowing the vehicle to be quickly adapted and optimized for a particular situation or mission. Figure 2 shows one configuration (b) opimized for speed and power, while the other (a) is optimized for mobility. For the 2000 competition, we have chosen configuration (a).

2.2 Farings

The fore and aft flooded 14" farings provide a more streamlined flow around the vertical motors and the frame. Additionally, the farings offer structural support and protection to any sensor mounted within them. Both farings are open on the top and bottom to provide for upward or downward looking sensors. Moreover, the forward section of the fore cone is open for any forward looking sensors.

2.3 Motors

All six motors are Motorguide Power Plus electric trolling motors with 6.75" diameter propellers. At 12V these motors provide approximately 22 pounds of thrust, and are fitted with custom O-ring seals that allow for a salt water depth of up to 100 feet. Each motor is shrouded to prevent incidental blade contact.

2.4 Through-hull connections

All through-hull connections use Burton 5500 series sealed and molded underwater connectors. A kill switch is implemented with a Giannini her-

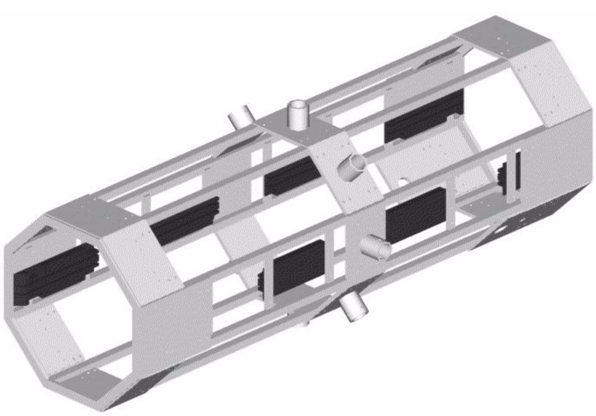

Fig. 1: Body frame

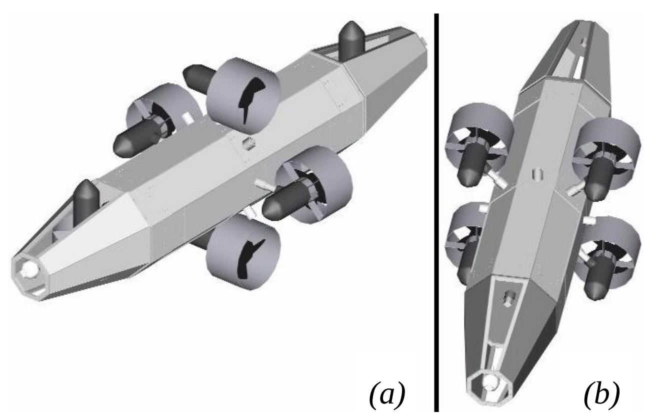

Fig. 2: Example configurations

metically sealed push-pull switch which disconnects power to the motors.

2.5 Interior layout

Two shelves guided on delrin rails provide support for all the internal electronics and power. Batteries and high-power electronics are stowed in the lower shelf to provide a metacentric righting-moment, while the upper shelf houses the remaining electronics. Electrical connections terminate at connectors at the back of the sub for expedient removal of both shelves.

3. Electrical System

The electrical system of the vehicle is composed of a power system (batteries and motor drivers), computing resources (x86 processor, microcontroller and DSP) and the sensors which provide information about the environment to the vehicle.

3.1 Power supply

SubjuGator uses five Powersonic 12 Amp-Hour 12V sealed lead-acid batteries, four to power the motors, and a one to power the electronics. A Wall Industries DC-DC converter supplies 5V at 4A for the electronics. This configuration allows for 3.5 to 4 hours operational runtime.

3.2 Computing

The various tasks of the computing system on SubjuGator demand different approaches. First, the motor system requires a consistent and dependable output to control motor speed. Second, the acoustic ping location system requires high-speed data acquisition, while the image processing system simply requires a powerful processor. To service these systems we chose the Motorola 68HC11, the Motorola DSP56309 Digital Signal Processor, and the WinSystems LBC-586Plus embedded single-board computer, respectively.

3.2.1 68HC11

The Motorola 68HC11 is an eight-bit microcontroller unit with flexible and powerful on-chip peripheral capabilities. These include an eight-channel analog-to-digital (A/D) converter with eight bits of resolution, an asynchronous serial communications interface (SCI), and five output-compare lines. The A/D converter, together with the SCI system, interfaces analog sensors to the digital main processor. The SCI system also receives motor output specifications, which are fed to the output compare lines to generate exact speed control for the motors.

3.2.2 Digital signal processor

The Motorola DSP56309 is an 80MHz 24-bit fully pipelined DSP. Of the many features of this system, the ones we are exploiting are (1) a serial communications interface, (2) system interrupt timer pins, and (3) a data acquisition time resolution of 27ns. The system interrupt timer pins extract phase information from the acoustic localization system to determine the bearing to the beacon. The SCI system receives instructions from the main processor, and transmits said phase information to the main processor.

3.2.3 Main processor

Top-level control is handled by a WinSystems LBC-586Plus single-board computer with 32MB RAM, running Red Hat Linux. This processor has the additional task of operating a parallel port camera and processing the images in search of a target hoop. All sensor information, now gathered on one system, is evaluated, and consequent instructions are then issued to all subsystems.

3.2.4 Wireless system access

A communications interface between a base station and the vehicle utilizes a wireless ethernet (IEEE802.11) connection with a 1.2Mb/s datapath. This allows telnet, ftp, and simultaneous programmer access for parallel code development and debugging.

3.3 Navigational sensors

For even the most basic operation, an AUV must be able to maintain a heading, a depth, an altitude and attitude. Sensors to allow this are present on almost all AUVs, regardless of any specific mission. We define these as navigational sensors.

3.3.1 Digital compass

SubjuGator uses a TCM2 compass from Precision Navigation. With a triaxial magnetometer, a fluidic inclinometer, and a microprocessor, this compass generates heading, tilt and roll information throughout its operational range.

3.3.2 Depth sensor

Depth measurements are gathered with a Measurement Specialties MSP-300 series pressure sensor. It is rated to 100 PSIG with a rated accuracy of $\pm 1\%$ and outputs an analog voltage between 1 and 5 volts, which translates to a depth resolution of ± 2 inches.

3.3.3 Sonar altimeter

We acquire height measurements with a Datasonics PSA-916 sonar altimeter. This model is modified to measure distances from 30cm to 100m with a resolution of 1cm over an RS-232 connection.

3.4 Mission-specific sensors

The competition task requires the localization and retrieval of a hoop located near a beacon emitting periodic acoustic and visual pulses. A secondary mission objective is to determine the period of the individual signals. Due to the dissimilar nature of the three "marking" methods, we have designed three sensors to allow us to completely achieve the mission goals.

3.4.1 CdS strobe detector

We accomplish the detection, localization and frequency determination of the strobe light through a series of light sensors and specialized circuitry. The sensors are twelve cadmium-sulfide (CdS) photoresistors which react to light by changing electrical resistance. They are arranged around the perimeter of the sub to effect coverage of most of the surrounding water. Figure 3 indicates the coverage provided by the arrangement of four sensors front and back and two on either side of the vehicle.

When designing the strobe detection hardware, environmental noise was a major consideration. In particular, the circuitry must detect a single flash from the strobe in an environment with varying ambient light and possible reflections from the sun off the water. Since a flash is basically a high frequency signal, we designed the sensor and circuitry combination to reject changes in light with a frequency less then 30kHz, a frequency threshold which we determined experimentally. The result is a calibration-free sensor that can detect and localize flashes in an environment where ambient lighting varies significantly.

The CdS sensors are Clairex CL5M7 hermetically sealed protoresistors. While the sensor circuitry can handle a wide range of photoresistors, we chose this model specifically because of the sealed packaging of the device. To adjust the field of view of each sensor, the photoresistors are collimated using a variable-length shroud. The amount of collimation is based on the mission objectives and operating environment of the vehicle.

3.4.2 Passive acoustic localization

3.4.2.1 System overview

The acoustic localization system consists of a passive hydrophone array that is tuned to the frequency of the beacon. With each received acoustic pulse, the array is able to calculate the bearing to the pinger relative to the AUV. The system utilizes three major components: a five-element hydrophone array, signal-detection circuitry, and a digital signal processor (DSP). The system is able to calculate a direction vector to a sound source (in this case an acoustic pinger) by measuring the phase difference of the signal of interest between a set of hydrophones with a fixed geometry.

3.4.2.2 Hydrophone array

Figure 4 illustrates the basic geometry of the hydrophone array. The hydrophone spacing is parameterized by *d*, the distance between the corner hydrophone, $H0$, and its two adjacent hydrophones, $H1$ and $H3$. The distance between $H1$ and $H2$, and between $H3$ and $H4$ is *3d/2*. This creates fixed relationships for the delay times be-

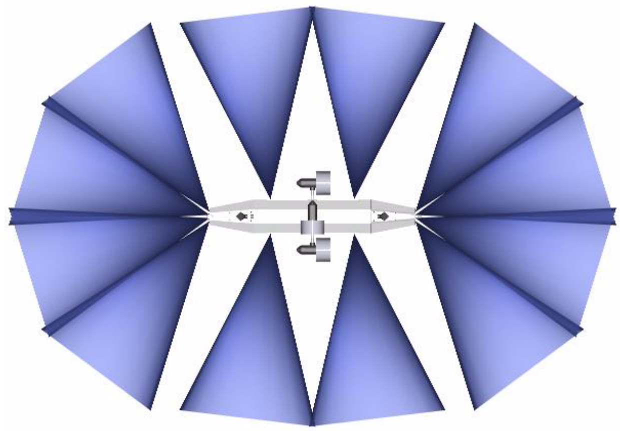

Fig. 3: CdS array

tween hydrophones on the same axis (i.e., $H0$, $H1$, and $H2$), which are exploited by the algorithm. It is very important for *d* to remain smaller than one full wavelength of the measured signal to prevent aliasing on the output vector. The array hydrophones are custom-designed International Transducers part ITC-4155. They are omnidirectional in their horizontal plane, and their sensitivity at 27kHz is close to -198dBV referenced to 1μPa.

3.4.2.3 Signal-detection circuitry

To measure the phase difference between two signals, a distinguishable common point must be chosen so that the time delay measurements will be accurate. A convenient point is the negative-going zero-crossing of a sinusoid (Figure 5). Specialized circuitry takes care of extracting the exact zero-crossing time for each signal. We amplify and filter raw hydrophone data before phase information can be extracted, as illustrated in Figure 6.

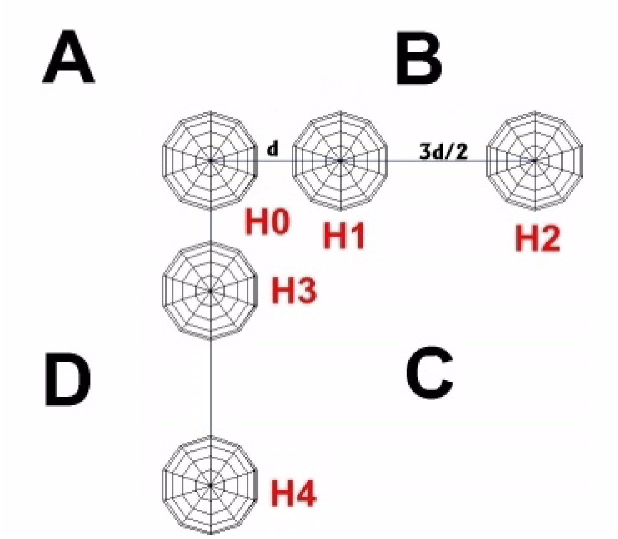

Fig. 4: Hydrophone array

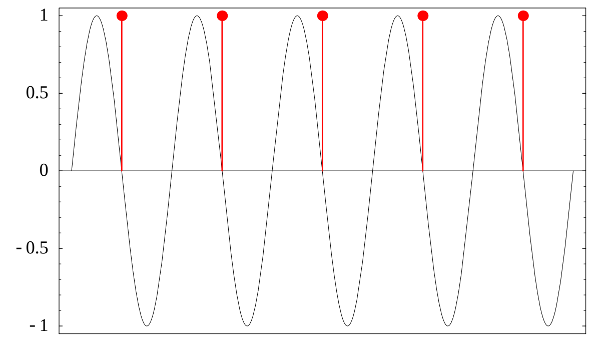

Fig. 5: Zero-crossing detection

Given the beacon power output of 174dB re 1μPa, the hydrophone sensitivity of -198dBV re 1μPa, and neglecting attenuation due to the small size of the pond, the output of each hydrophone will be $0.05mV_{p\text{-}p}$. An instrumentation amplifier with a gain of 20 will sufficiently amplify this voltage to a suitable level for filtering. The small scale of the hydrophone output stresses the importance of using high-quality instrumentation amplifiers which will reject common-mode noise and provide wide bandwidth. The amplifier is an Analog Devices AD623.

The wide-band amplified signal now passes through a fourth-order Chebyschev bandpass filter to eliminate out-of-band noise. The filter has a center frequency of 27kHz and bandwidth of 2kHz. A Maxim MAX268 provides a single-chip filtering solution. At the passband, the filter has a gain of 100, generating an output voltage large enough for zero-crossing detection.

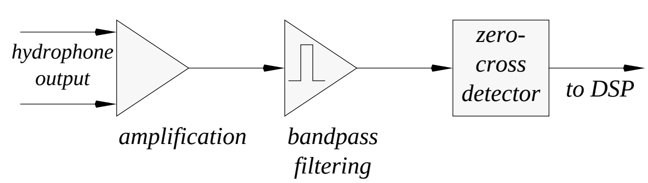

Fig. 6: Signal detection

A National Semiconductor LM1815 variable reluctance sensor amplifier acts as a zero-crossing detector. It triggers only on signals greater than 200mV peak, rejecting almost all of the noise that is not sufficiently attenuated by the filter. The output is a quick (7 µs) voltage pulse, which is fed into the DSP for processing.

3.4.2.4 Digital signal processor

The signal-detection circuitry described above transforms the output of the hydrophones into periodic pulses representing the zero-crossing points of the acoustic signal from the beacon. Since these pulses are about 37 microseconds apart (one period of a 27kHz sinusoid), the measured phase difference (time between zero-crossing for two hydrophones) will range from 0 to 37µs. During each 5 millisecond pulse the DSP captures 128 data points (phase difference measurements) per hydrophone. This large number of samples helps to discard anomalous readings, and gives some measure of confidence for the direction vector (i.e., how many of the readings agree with each other).

3.4.2.5 Algorithm and output

Four data points corresponding to time delays are input to the algorithm: t_1 and t_2 are the phase difference between $H0$ and $H1$, and $H0$ and $H3$, respectively; t_3 and t_4 are the delays between $H1$ and $H2$, and $H3$ and $H4$, respectively. We break up the space around the array into octants, letting $H0$ be the origin, the $H0$-$H3$-$H4$ line be the x-axis, and the $H0$-$H1$-$H2$ line be the y-axis. We shall further assume that signals will only be received from *below* the array (i.e., only signals with negative z-axis values), a sensible assumption, since we know the beacon is on the bottom of the lake. This reduces the space into four "octants", which we label A, B, C and D as shown in Figure 4.

Given these definitions, there are four possible sets of relationships between t_1 and t_3, and t_2 and t_4, depending from which octant the signal originated. Table 1 shows these relationships, where τ is the period of the 20kHz signal.

The source octant is determined by comparing the measured values of t_3 and t_4, to the calculated values from Table 1. The winning octant is that with the smallest difference between t_3 and t_4. After determining the source octant, we can calculate two angles, θ_α and θ_β, which are the angles with the $X-Z$ and $Y-Z$ planes, respectively, of a vector in the direction of the sound source. To compute these angles we refer the reader to Tables 2 and 3 in [1].

Octant A	*Octant B*
$t_3 = \begin{cases} 3t_1/2 \\ 3t_1/2 - \tau \end{cases}$ $t_4 = \begin{cases} 3t_2/2 \\ 3t_2/2 - \tau \end{cases}$	$t_3 = \begin{cases} (3t_1 + \tau)/2 \\ (3t_1 - \tau)/2 \end{cases}$ $t_4 = \begin{cases} 3t_2/2 \\ 3t_2/2 - \tau \end{cases}$
Octant D	*Octant C*
$t_3 = \begin{cases} 3t_1/2 \\ 3t_1/2 - \tau \end{cases}$ $t_4 = \begin{cases} (3t_2 + \tau)/2 \\ (3t_2 - \tau)/2 \end{cases}$	$t_3 = \begin{cases} (3t_1 + \tau)/2 \\ (3t_1 - \tau)/2 \end{cases}$ $t_4 = \begin{cases} (3t_1 + \tau)/2 \\ (3t_1 - \tau)/2 \end{cases}$

Table 1: Phase relationships for each octant

3.4.3 Vision-based ring detection

A Connectix Quickcam greyscale camera, mounted in the nose cone of the sub, collects forward-looking images. The camera quantizes pixels to 64 shades of grey, and has software-adjustable contrast and brightness settings. Processing of the images is handled in three steps: (1) preprocessing, (2) segmentation, and (3) ring detection.

3.4.3.1 Image preprocessing

To account for varying lighting conditions, the brightness setting on the camera is dynamically adjusted to provide an image with a pre-defined average brightness level. The resulting image is then thresholded to a binary pixel-map. Figure 7 shows an image collected, and preprocessed.

3.4.4 Image segmentation

The preprocessed image is analyzed to extract features, which are defined to be groupings of white-connected pixels. We then store each feature and its critical dimensional information in a list. We define a features critical dimensional information to be the coordinates that indicate a bounding box for the feature, and a total pixel count for the feature. The list allows for quick referencing in later processing steps.

3.4.4.1 Ring detection

A recognizable ring in an image exhibits three distinguishing properties. Measured along a line through the center of the hoop, the thicknesses of a "leg" along the hoop's major (horizontal) and minor (vertical) axes are invariant with respect to the aspect ratio. Each thickness does not cover more than two-thirds the major or minor axis length, and the aspect ratio (major axis length divided by minor axis length) of a ring is never greater than 1.0 when the line of sight of the viewer is perpendicular to the face of the ring. We have constructed an algorithm that eliminates non-ring features from the list when they do not exhibit the above discussed properties. A distinct advantage of the algorithm over using parametric equations is that false positive identification (a ring mistaken for a non-ring feature) is less of an issue when analyzing an image containing a partial ring (Figure 8).

We further refine the list by comparing the thicknesses along the major and minor axes of the remaining features. The feature with the minimum average thickness difference is identified as the ring, along with a confidence measure defined as,

$$\frac{\text{minor axis length} - \text{avg. difference}}{\text{minor axis length}} \tag{1}$$

If the above procedure results in a null list, the ring-detection algorithm returns zero. In Figure 9, we show one example of a successful ring detection, and one example of a successful ring rejection. The first sequence picks out the ring from the image by successful removal of non-ring features. The second sequence shows a cluttered environment with no ring. The algorithm rejects every feature in the image, and no ring is found.

4. Vehicle control and mission strategy

4.1 PID controller

As the submarine moves through the water, errors between the desired and current values of heading, speed, pitch, and depth will be controlled through a standard PID controller. The determination of the motor actuation values is based on the submarine's position and orientation divergence according to,

$$m(t) = K_p e(t) + K_i \int_0^t e(\tau) d\tau + K_d \frac{de(t)}{dt} \tag{2}$$

where $m(t)$ is the motor value and $e(t)$ represents the error at time step t. The continuous equation is converted to its discrete-time equivalent and the

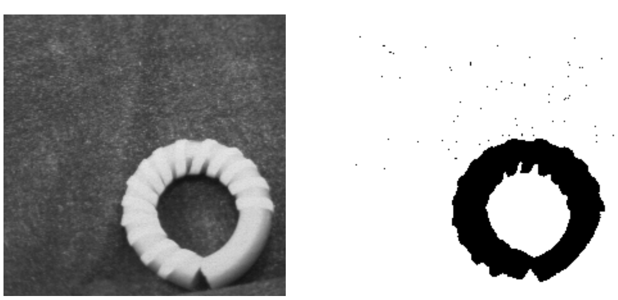

Fig. 7: Image preprocessing

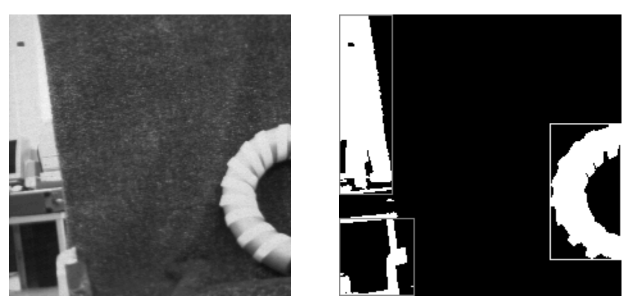

Fig. 8: Partial ring detection

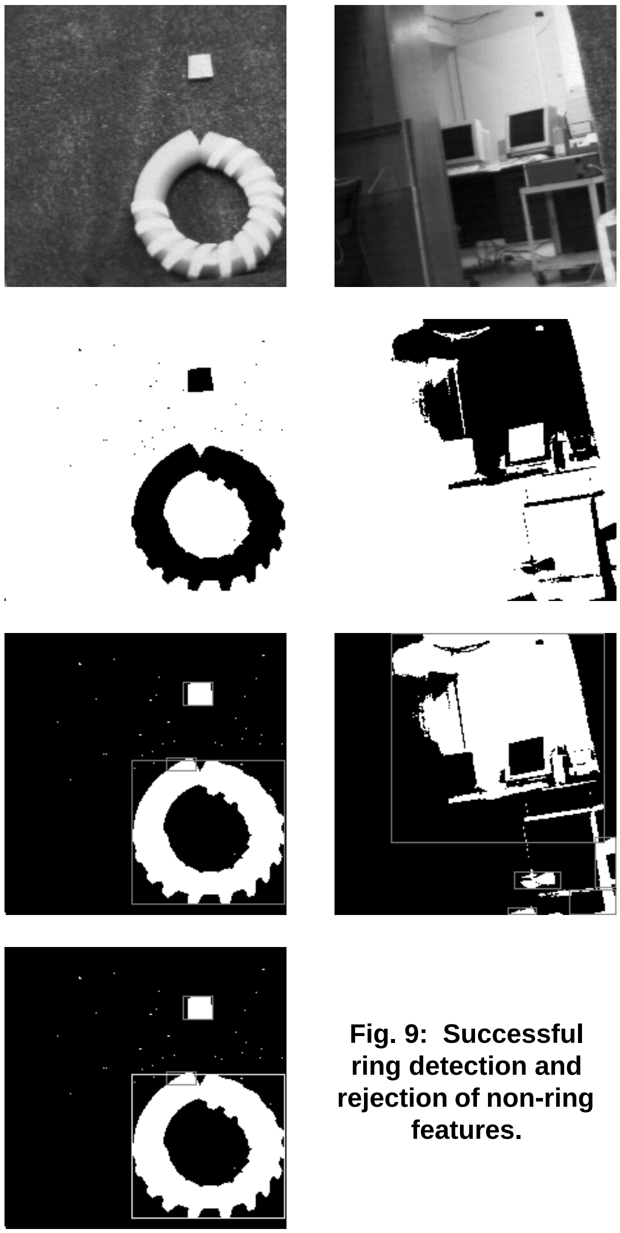

Fig. 9: Successful ring detection and rejection of non-ring features.

errors are calculated from the difference between the current and desired heading, pitch and depth.

Manually tuning the gains in equation (2) above can involve much trial-and-error. In order to short-circuit this process, we have implemented *Q*-learning [2] to automatically tune the gains to achieve the best response over time. We allow the submarine to explore different gain combinations and reward those with desirable control properties such as small overshoot and fast response time. This is not only a painless alternative to manual fine tuning, but also offers an automated procedure for adjusting the gains, if the mechanical parameters of the submarine are changed or redesigned.

4.2 Arbiter

Each of the sensor analysis processes make heading, speed and depth requests to improve the position of the sub in relation to the beacon. Due to the various strengths and weaknesses of particular sensors, and the occasional sensor anomaly, these requests may sometimes conflict. Therefore, we have implemented an arbiter, a rule-based algorithm specifically created for the competition environment, which is tasked with deciding on the next action for the sub, given the various, possibly erroneous, sensor inputs.

We describe a hypothetical successful mission run below. The hydrophone array will detect the beacon ping, and derive a heading to the beacon. Knowledge about the current depth of the vehicle and the maximum pond depth will be used to estimate the maximum possible distance to the beacon. As the vehicle approaches the beacon, the CdS array should detect and localize a flash. If these two sensors agree concerning the beacon bearing, the vehicle will continue on its path and await the vision- based hoop detector to recognize a target. When the vision system finds a hoop, it will then be permitted to adjust the sub position for target retrieval.

This sequence allows for each sensor to contribute where it is most effective, without having to rely exclusively on one sensor alone. It is likely, for example, that the camera system will detect the hoop of an inactive beacon during a run. If the CdS and hydrophone systems report a beacon bearing that is not currently in the line-of-sight of the camera, the false target is ignored. The CdS and hydrophone arrays will continuously compare beacon bearing estimates to maximize confidence for a chosen action. This "sensor overlap" provides a measure of robustness in the detection sequence that we believe offers a good chance for a successful mission.

5. Acknowledgements

We thank our sponsors: Harris Semiconductors, UF College of Engineering, UF Dept. of Electrical Engineering, International Transducer Corporation, Burton Electrical Engineering, Giannini, Torpedo Industries, Precision Navigation, UF Dept. of Chemistry Machine Shop. We would like to especially thank Todd Prox of the Chemistry Machine Shop for his time and expertise. Thanks to our faculty advisors who protected us from the paper storm that is inevitable with such a project.

6. References

[1] US patent 4,622,657, "Acoustic Direction Finding Systems," Nov. 11, 1986.

[2] C. J. Watkins, *Learning from Delayed Rewards*, Ph.D. Thesis, King's College, Cambridge, UK, 1989.